Biomedicine & Pharmacotherapy 173 (2024) 116331

Contents lists available at ScienceDirect

Biomedicine & Pharmacotherapy

journal homepage: www.elsevier.com/locate/biopha

Improvement of NASH and liver fibrosis through modulation of the gut-liver axis by a novel intestinal FXR agonist

An-Na Moon [a,b], François Briand [c], Natalia Breyner [c], Dong-Keun Song [b], Martin Rønn Madsen [d], Hongbin Kim [e], Keonwoo Choi [e], Yoonsuk Lee [b,*], Wan Namkung [a,**]

[a] College of Pharmacy and Yonsei Institute of Pharmaceutical Sciences, Yonsei University, 85 Songdogwahak-ro, Yeonsu-gu, Incheon 21983, South Korea
[b] iLeadBMS Co., Ltd., 614 Dongtangiheung-ro, Hwaseong-si 18469, South Korea
[c] Physiogenex, 280 rue de l'Hers, ZAC de la Masquère, Escalquens 31750, France
[d] Gubra, Hørsholm Kongevej 11B, Hørsholm 2970, Denmark
[e] KINS, Korean Institute of Nonclinical Study, 172 Dolma-ro, Bundang-gu, Seongnam-si, Gyeonggi-do 13505, South Korea

ARTICLE INFO

Keywords:
NASH
FXR
Gut
Bile acid
Microbiota
Pruritus

ABSTRACT

Farnesoid X receptor (FXR) plays a pivotal role in the regulation of bile acid homeostasis and is involved in the pathogenesis of nonalcoholic steatohepatitis (NASH). Although FXR agonists effectively alleviate pathological features of NASH, adverse effects such as disturbance of cholesterol homeostasis and occurrence of pruritus remain to be addressed. Here, we identified a novel FXR agonist, ID119031166 (ID166), and explored the pharmacological benefits of ID166 in the treatment of NASH. ID166, a potent and selective non-bile acid FXR agonist, exhibits preferential distribution in the intestine and shows no agonist activity against potential itch receptors including Mas-related G protein-coupled receptor X4 (MRGPRX4). Interestingly, ID166 significantly attenuated total nonalcoholic fatty liver disease (NAFLD) activity and liver fibrosis in a free choice diet-induced NASH hamster model. In addition, ID166 drastically modulated the relative abundance of five gut microbes and reduced the increase in plasma total bile acid levels to normal levels in NASH hamsters. Moreover, long-term treatment with ID166 significantly improved key histological features of NASH and liver fibrosis in a diet-induced NASH mouse model. In the NASH mouse livers, RNA-seq analysis revealed that ID166 reduced the gene expression changes associated with both NASH and liver fibrosis. Notably, ID166 exhibited no substantial effects on scratching behavior and serum IL-31 levels in mice. Our findings suggest that ID166, a novel FXR agonist with improved pharmacological properties, provides a preclinical basis to optimize clinical benefits for NASH drug development.

1. Introduction

Over the last decade, nonalcoholic steatohepatitis (NASH) has emerged as a major indication for liver transplantation (LT) in non-hepatocellular carcinoma (HCC) patients, with a significant prevalence of comorbidities such as obesity and diabetes.[1] NASH imposes a substantial burden on clinical management due to the remarkably elevated prevalence of comorbidities such as obesity, diabetes, and hypertension.[2] Along with the increased risk of early-onset obesity and type 2 diabetes, there has also been a dramatic rising trend of nonalcoholic fatty liver disease (NAFLD) in the younger population.[3] The NAFLD is the most common liver disease worldwide and ranges from simple steatosis to more severe liver diseases with fibrosis such as NASH.[4] Despite the global need for NASH treatment, there are currently no Food and Drug Administration (FDA) approved drug for NASH. Therefore, nonclinical and clinical approaches should be

Abbreviations: FXR, farnesoid X receptor; ID166, ID119031166; BA, bile acid; MRGPRX4, Mas-related G protein-coupled receptor X4; TGR5, Takeda G-protein-coupled receptor 5; ALT, alanine aminotransferase; AST, aspartate aminotransferase; *Shp*, small heterodimer partner; *Bsep*, bile salt export pump; *Cyp8b1*, cytochrome P450 Family 8 Subfamily B Member 1; C4, 7α-hydroxy-4-cholesten-3-one; CDCA, chenodeoxycholic acid; CA, Cholic acid; DCA, deoxycholic acid; LCA, Lithocholic acid; TDCA, taurodeoxycholic acid; GDCA, glycodeoxycholic acid; TCDCA, taurochenodeoxycholic acid; GCDCA, glycochenodeoxycholic acid; TCA, taurocholic acid; GCA, glycocholic acid; HFHC, high fat diet/high cholesterol; DNCB, 2,4-dinitrochlorobenzene; CETP, cholesteryl ester transfer protein.

* Corresponding author.
** Correspondence to: College of Pharmacy and Yonsei Institute of Pharmaceutical Sciences, Yonsei University, Incheon 21983, South Korea.
E-mail addresses: ivo.lee@ileadbms.com (Y. Lee), wnamkung@yonsei.ac.kr (W. Namkung).

https://doi.org/10.1016/j.biopha.2024.116331
Received 29 November 2023; Received in revised form 21 February 2024; Accepted 22 February 2024

attempted to develop effective NASH treatments.

Farnesoid X receptor (FXR), a bile acid receptor, is activated by endogenous bile acids such as chenodeoxycholic acid (CDCA).[5] FXR is predominantly enriched in tissues such as the liver and intestines, where it plays a pivotal role in regulating bile acid homeostasis during the enterohepatic cycling process. FXR is also known as a nuclear receptor that binds to DNA as a heterodimer with its common partner, retinoid X receptor (RXR).[6] The activation of FXR initiates the release of co-repressors and recruitment of co-activators, which regulate the transcriptional activation or repression of downstream genes associated with NASH.[7,8] FXR has been identified as a potential druggable therapeutic target for NASH. In phase 3 clinical trial for NASH, obeticholic acid (OCA), a steroidal FXR ligand, demonstrated clinical efficacy by eliciting histological improvement. However, due to serious safety risks, full confirmation of its clinical benefit was not achieved.[9] The development of non-steroidal FXR agonists with a differentiated pharmacological profile has emerged as a potential strategy to overcome the limits imposed by steroid structure. However, most non-steroidal FXR agonists in the clinical stage mainly aim at liver-distributed systemic therapy and struggle with insufficient efficacy.[10,11] Interestingly, a previous study showed that fexaramine, a novel FXR agonist that exhibits gut-restricted capacity, is effective in improving metabolic dysregulation by reducing diet-induced weight gain, hepatic glucose production, and body-wide inflammation without activation of hepatic FXR target genes.[12] Although no clinical trials have been conducted on the effectiveness of fexaramine, a novel fexaramine-derived FXR agonist, MET-409, has been studied clinically for NASH. However, MET-409 focused on sustained systemic pharmacokinetic (PK) properties and showed common side effects at effective doses in the NASH trial.[13,14] Therefore, intestinal FXR agonist has not yet been tested in NASH patients, and tissue-specific FXR agonists are expected to provide a novel therapeutic strategy for NASH by mitigating the adverse effects of long-term systemic exposure.

Recent studies have focused on elucidating changes in the gut microbiome and their implications in metabolic diseases, including NAFLD.[15] The taxonomic composition of the gut microbiome has been found to be associated with the severity of NAFLD at the familial level, and NASH patients also show changes in the abundance of several bacteria, including *Bacteroides* and *Prevotella*.[16] In mice, the gut microbiota is known to have a significant impact on secondary bile acid metabolism and bile acid profiles, affecting FXR activity.[17] However, it remains unclear whether non-bile acid FXR agonists alter the diversity and composition of the gut microbiota in NASH hamsters.

In this study, we identified a novel non-bile acid FXR agonist, ID166, preferentially distributed to intestine,[18] and investigated the effects of ID166 on key histological features, liver fibrosis, plasma bile acid levels, gut microbiota, and gene expression profiles in hamster and mouse NASH models.

2. Materials and methods

2.1. Chemicals

ID166, IUPAC name (5-((2-Chloro-4-((5-cyclopropyl-3-(2,6-dichlorophenyl)isoxazol-4-yl)methoxy)phenyl)ethynyl)−2-cyclopropylbenzo[*d*]oxazole-7-carboxylic acid), was synthesized in five chemical steps at Sundia Meditech Co., Ltd (Shanghai, China). Each batch was prepared as the free base at a purity of greater than 98%. The synthesis and representative chemical characterization details are described in the Supplementary Material. Obeticholic was sourced from a commercial supplier (MedKoo Bioscience, NC, USA). Tropifexor and Cilofexor were purchased from MedChemExpress (NJ, USA). Lithocholic acid, deoxycholic acid and other bile acid species were purchased from Sigma-Aldrich (MO, USA). MS47134 was synthesized under the modified conditions previously reported.[19]

2.2. In vitro FXR activity and selectivity

FXR ligand binding domain (Invitrogen, USA) and SRC1 peptide (GL Biochem, China) were used to perform TR-FRET FXR co-activator recruitment assay at ChemPartner (Shanghai, China). Nuclear receptor reporter assays were conducted at Indigo Bioscience (PA, USA). GPCR functional assays for TGR5 and MRGPRX4 were performed at Multispan (CA, USA). Human hepatocyte assay was conducted at BioDuro-Sundia (Shanghai, China). Further experimental details are provided in Supplemental Material.

2.3. Pharmacokinetic and pharmacodynamic studies in normal hamsters

Animal experiments were performed at Physiogenex (Escalquens, France). The bioanalysis for plasma and tissue samples was conducted at Eurofins ADME BIOANALYSES (Vergeze, France). After the acclimation period, hamsters were randomized into the treatment groups. The hamsters were then treated orally once daily with vehicle or ID166 at 3, 10, 20 and 30 mg/kg for 14 days. All animal protocols were reviewed and approved by the local (Comité régional d'éthique de Midi-Pyrénées) and national (Ministère de l'Enseignement Supérieur et de la Recherche) ethics committees (protocol number CEEA-122–2014–15). Other details are provided in Supplemental Material.

2.4. Animal models of NASH

Male golden Syrian hamsters and C57Bl6/J mice were utilized to generate diet-induced NASH models at Physiogenex (Escalquens, France). After 15 or 22 weeks of free choice diet, hamsters were kept on diet and treated with vehicle, ID166 at 10 or 30 mg/kg orally once daily for 5 weeks. After 7 weeks of high fat diet/high cholesterol diet, mice were kept on diet and treated with vehicle and ID166 at 15 or 50 mg/kg orally once daily for 18 weeks. All animal protocols for NASH models were reviewed and approved by the local (Comité régional d'éthique de Midi-Pyrénées) and national (Ministère de l'Enseignement Supérieur et de la Recherche) ethics committees (protocol number CEEA-122–2014–15). Further details are provided in Supplemental Material.

2.5. Metagenomic sequencing of fecal microbiota in hamsters

The relative proportion of 16 S rDNA bacterial taxa in the fecal samples of normal and NASH hamster was determined using next generation high throughput sequencing of variable regions of the 16 S rRNA bacterial gene at Vaiomer (Labège, France). Other details are provided in Supplemental Material.

2.6. Bile acid and C4 analysis

Bile acids (BA) and C4 (7α-hydroxy-4-cholesten-3-one) analysis was performed at the mass spectrometry platform led by Dr. Antonin Lamazière, Sorbonne Université (Paris, France). BA were purified by solid phase extraction and measured, using a QTRAP® 2000, high-pressure liquid chromatography and tandem mass spectrometry system (Applied Biosystems/MDS SCIEX, Concord, Ontario, Canada). The C4 extraction method was similar to the bile acids extraction and the serum C4 quantification was performed using a deuterated C4 form as internal standard (7α-hydroxy-4-cholesten-3-one-d7). Further details are provided in Supplemental Material.

2.7. RNAseq analysis

RNA sequencing (RNAseq) was conducted using RNA extracts from mouse liver and ileum samples at Gubra (Hørsholm, Denmark). RNA sequence libraries were prepared from liver tissue with the NeoPrep system (Illumina, San Diego, CA) using Illumina TruSeq stranded mRNA Library kit for NeoPrep (Illumina) and sequenced on the NextSeq 500

(Illumina) with NSQ 500 hi- Output KT version 2 (75 CYS; Illumina). Reads were aligned to the GRCm38 version 96 Ensembl Mus musculus genome default parameters. Differential gene expression analysis was performed using DESeq2 including Benjamin-Hochberg correction for multiple testing.

2.8. Animals for cutaneous examination

All animal procedures for cutaneous examinations were approved by the Institutional Animal Care and Use Committee (IACUC) of the Seoul National University Bundang Hospital (IACUC No. BA-2208–349–004–03). 7-week-old BALB/c mice were treated with vehicle and ID166 at 50 mg/kg orally once daily for 4 weeks. Other details are provided in Supplemental Material.

2.9. Statistical analyses

Statistical analysis was performed using GraphPad Prism (version 9) using a One-way ANOVA with Dunnett's post-test or a Kruskal-Wallis with Dunn's post-test in case of significant variance. Additionally, an Unpaired t-test or a Mann-Whitney test was employed when comparing one single treatment group with the vehicle group. A significance level of $p < 0.05$ was considered statistically significant.

3. Results

3.1. ID166, a novel FXR agonist, potently and selectively activates FXR in vitro and in vivo

To identify a novel chemical series of non-bile acid FXR agonists, we introduced both a triple bond as a novel middle liker and the terminal benzoxazole moiety whereas we conserved the widely investigated trisubstituted isoxazole core compound moiety which so-called "hammerhead" class by GlaxoSmithKline.[20,21] The agonistic activities of novel compounds were screened using a CHO cell-based FXR reporter assay. As shown in Fig. 1A, the *in vitro* potency of ID166 was confirmed using TR-FRET FXR co-activator assay (EC_{50} of 3 nM) and FXR reporter assay (EC_{50} of 5 nM). We also performed the computational modeling simulation of ID166 to predict its potential modes of interactions with FXR ligand binding domain (LBD). ID166 resides in a hydrophobic pocket of the FXR-LBD (PDB 3DCT) and its terminal benzoxazole moiety interacts with the chains of Arg 331 and Met 265 via

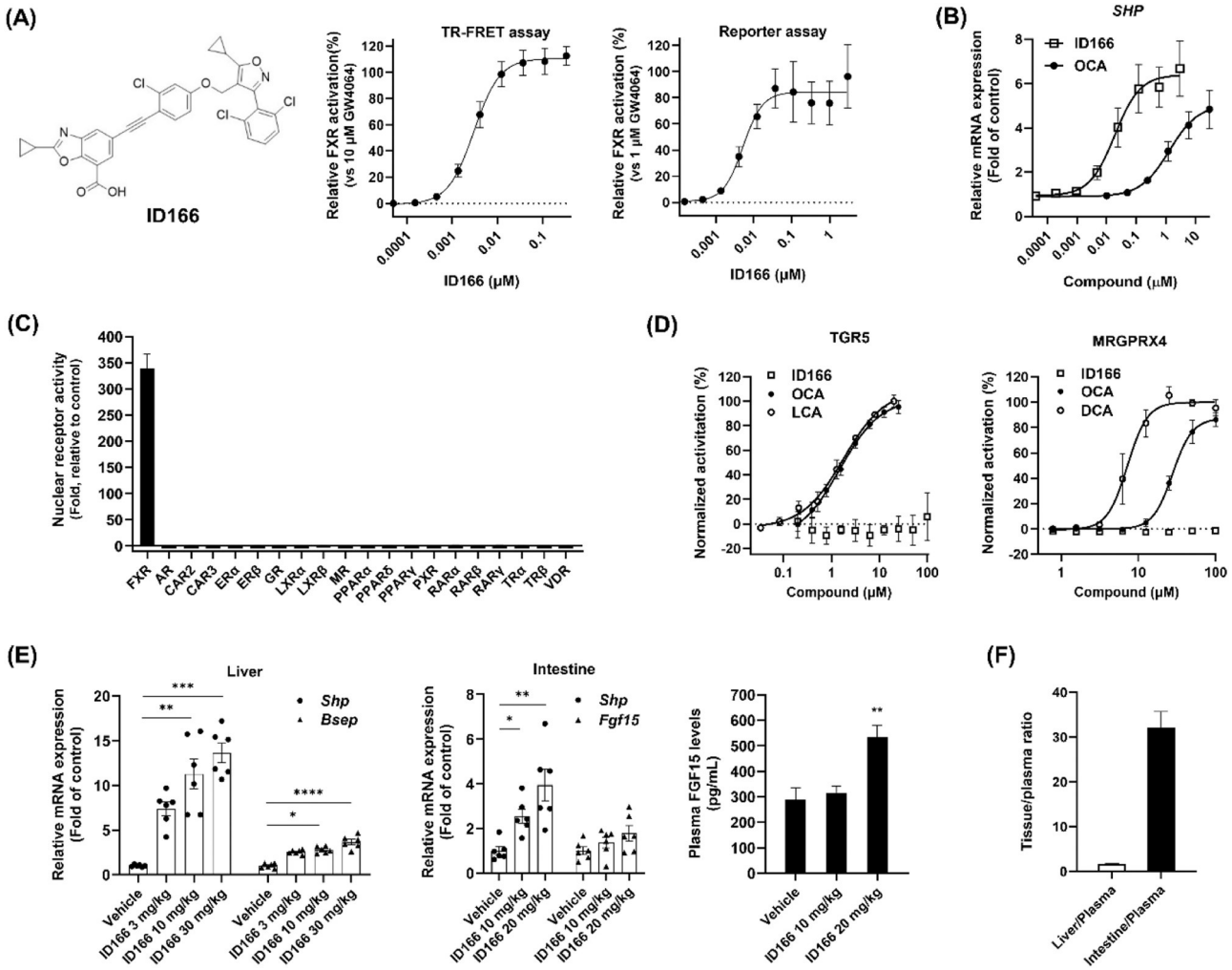

Fig. 1. Structure and pharmacological profile of ID166. (A) Structure and dose-response curves of ID166, a novel FXR agonist (mean ± SD, *n=9*). (B) Relative mRNA levels of *SHP* gene induced by FXR agonists in primary human hepatocytes (mean ± SEM, *n=9*). (C) Nuclear receptor activities of ID166 at 3 μM were determined using luciferase reporter assays by Indigo Bioscience (mean ± SD, *n=3*). (D) The dose-response curves of ID166 and reference agonists for human TGR5 and MRGPRX4 (mean ± SD, *n=6*). (E) The relative mRNA expression of FXR target genes in normal hamster liver and intestine was also determined by qPCR after 14-day repeated oral administration of ID166 (mean ± SEM, *n=6*). Plasma FGF15 levels in the normal hamsters were measured on day 14 at 6 h post-dose (mean ± SEM, *n=6*). (F) Tissue-to-plasma ratio at 2 h post-dose following 14 days of oral administrations of 30 mg/kg/day ID166 in normal hamsters (mean ± SEM, *n=3*). Significance was determined by Kruskal-Wallis with Dunn's post-test vs vehicle. $^{*}p < 0.05$, $^{**}p < 0.01$, $^{***}p < 0.001$ and $^{****}p < 0.0001$ vs vehicle.

hydrogen bonding (Fig. S1). Subsequently, we conducted a pharmacological assessment of ID166 on primary human hepatocytes obtained from three different donors. To assess and compare the efficacy of ID166 and OCA in human primary hepatocytes, we investigated the effects of these agonists on gene expression levels of small heterodimer partner (*SHP*), a FXR target gene. When human hepatocytes were treated with the agonists for 24 h, ID166 induced *SHP* gene expression more strongly than OCA (EC_{50} of 1 μM) with an EC_{50} value of 19 nM (Fig. 1B). To examine the selectivity of ID166, we performed a luciferase reporter assay on 19 human nuclear receptors and found that ID166 is highly selective for FXR compared to other nuclear receptors up to 3 μM (Fig. 1C). To investigate the effects of ID166 on potential itch receptors, Mas-related G protein-coupled receptor X4 (MRGPRX4) and Takeda G protein-coupled receptor 5 (TGR5), we performed a cell-based assay and found that ID166 did not exhibit agonistic activities on either MRGPRX4 or TGR5 up to 100 μM (Fig. 1D).

To confirm that ID166 is applicable to the *in vivo* NASH model, ID166 was repeatedly orally administered to normal hamsters at different doses for 14 days. ID166 strongly increased the gene expression levels of the FXR target genes up to 14-fold in hamster liver and intestine in a dose-dependent manner, and plasma fibroblast growth factor 15 (FGF15) level was significantly increased by ID166 at a dose of 20 mg/kg/day (Fig. 1E). In addition, when ID166 was orally treated for 14 days in normal mice, ileal *Shp* and *Fgf15* gene expression also significantly increased in an ID166 concentration-dependent manner (Fig. S2). The distribution characteristics of ID166 between the intestines and liver were investigated in normal hamsters. Interestingly, ID166 exhibited a preferential distribution in the intestine. Notably, the average intestine-to-plasma ratio was 20-fold higher than the liver-to-plasma ratio (Fig. 1F).

3.2. ID166 alleviates diet-induced NASH phenotypes in hamsters

To further evaluate the effect of ID166 on the NASH phenotype, we utilized a diet-induced NASH hamster model that mimics human NASH and lipoprotein cholesterol metabolism.[22] After the 15-week diet induction period, NASH hamsters were given vehicle, ID166 10 and 30 mg/kg/day for 5 weeks under the continuous exposure to a free-choice diet (Fig. 2A). H&E and Sirius red staining showed that ID166-treated hamsters reduced the key phenotypic NASH features seen in vehicle-treated hamsters in a dose-dependent manner (Fig. 2B). Total NAFLD activity, steatosis and hepatocyte ballooning scores were significantly increased in NASH hamsters compared to normal controls and the increased NAFLD activity, steatosis and hepatocyte ballooning scores were strongly decreased by ID166 treatment in NASH hamsters (Fig. 2C). Notably, ID166 significantly reduced the Sirius red-stained fibrosis area at a dose of 30 mg/kg/day (Fig. 2D). Hepatic triglycerides levels were also decreased in ID166-treated NASH hamsters (Fig. 2E). To investigate the *in vivo* target engagement of ID166, we observed the gene expression levels of FXR target genes in NASH hamsters. In NASH hamsters, ID166 significantly increased the gene expression of *Shp* in the liver and intestine, as well as the bile salt export pump (*Bsep*) in the liver, while it led to a significant decrease in the expression of the liver *Cyp8b1* gene compared to the vehicle-treated group (Fig. 2F).

3.3. ID166 reduces total NAFLD activity score and liver fibrosis without plasma LDL-C elevation in NASH hamsters

Next, we examined the *in vivo* efficacy of ID166 on NASH hamsters fed a free choice diet for longer induction periods up to 22 weeks. In this NASH hamster model, the duration of free choice diet feeding promoted NASH features and liver fibrosis.[23] After 22 weeks of a free choice diet, vehicle and 30 mg/kg/day ID166 were subsequently administered to fifteen NASH hamsters for 5 weeks under a free choice diet (Fig. 3A). In contrast to the liver histology of control hamsters, severe liver fibrosis was observed in the 27-week free-choice diet NASH hamster model, and administration of ID166 strongly reduced the liver fibrosis in NASH hamsters (Fig. 3B). Notably, ID166 drastically improved not only total NAFLD activity but fibrosis scores compared to vehicle (Fig. 3C). To investigate the effects of ID166 on fibrogenic gene expression, we observed hepatic mRNA levels of tissue inhibitor of metalloproteinases 1 (*Timp1*), transforming growth factor beta 1 (*Tgfb1*) and collagen type III alpha 1 chain (*Col3a1*), and found that ID166 significantly reduced the elevated gene expressions of *Timp1*, *Tgfb1* and *Col3a1* in NASH hamster liver (Fig. 3D).

To assess hepatic damage in NASH hamsters, plasma levels of alanine aminotransferase (ALT) and aspartate aminotransferase (AST) were quantified. ID166-treated NASH hamsters showed a signification reduction of plasma ALT levels compared to vehicle-treated group. Notably, ID166 lowered the plasma ALT levels to levels comparable to those in control hamsters, and the plasma AST levels in ID166-treated group showed a tendency to be lower compared to vehicle-treated group (Fig. 3E). In human, cholesteryl ester transfer protein (CETP) mediates lipoprotein metabolism by transferring cholesteryl ester between vascular lipoproteins,[24] and Golden Syrian hamsters also have plasma CETP activity unlike mouse, rat and dog.[25] Considering the similarities in lipid-protein metabolism between humans and hamsters, we investigated whether ID166 exhibits beneficial effects on plasma lipid parameters. ID166 significantly reduced plasma LDL-C levels in NASH hamsters, while it had no effect on plasma TG, TC and HDL-C levels. Interestingly, hepatic TG levels, which were significantly increased in NASH hamsters, were significantly reduced by ID166 (Fig. 3F).

3.3. ID166 modulates the relative abundance of gut microbes in NASH hamsters

ID166 is preferentially distributed in the hamster intestine (Fig. 1F). Thus, we investigate whether ID166 could affect gut microbiota in NASH hamsters. The fecal samples were collected from NASH hamsters fed 15 weeks of free choice diet following 5-week treatment of vehicle and ID166. The control fecal samples were also harvested from normal hamsters fed a standard chow diet. Microbial populations of the fecal samples were estimated by using next generation high throughput sequencing of variable regions of the bacterial 16 S ribosomal RNA (rRNA) genes. We estimated the microbial alpha diversity to evaluate the alteration of the microbiota community structure between each group. Chao1 and Observed indices calculated the alpha diversity including species richness which means the number of taxa that are present in the samples. Simpson and Shannon indices represented the alpha diversity of taxa in the samples both in terms of richness and evenness. ID166 maintained the alpha diversity of gut microbes compared to the control at the family level (Fig. 4A), and the 15 most abundant bacteria were identified at the family level (Fig. 4B). Interestingly, we found distinct variations in the relative abundances of five bacteria at the genus level when exposed to ID166. Specifically, *Lactobacillus*, *Bifidobacterium,* and *Odoribacter* exhibited significantly higher abundances compared to the vehicle group, while *Prevotella* and *Bacteroides* displayed statistically lower abundances than the vehicle-treated group (Fig. 4C).

3.4. ID166 alters bile acid profiles in NASH hamsters

Elevated levels of plasma bile acids have been reported in patients with NASH and have been found to be associated with the severity of key components of NASH.[26,27] Thus, we investigated whether ID166 altered plasma bile acid signatures in NASH hamsters. At 27 weeks of a free choice diet, we collected plasma samples at 4 h post-dose to analyze bile acid levels in NASH hamsters. The control plasma samples were also harvested from normal hamsters fed a chow diet.

Although there were variations in plasma total, unconjugated, and conjugated bile acid levels between individual hamsters, ID166 significantly decreased the plasma concentrations of total, unconjugated, and

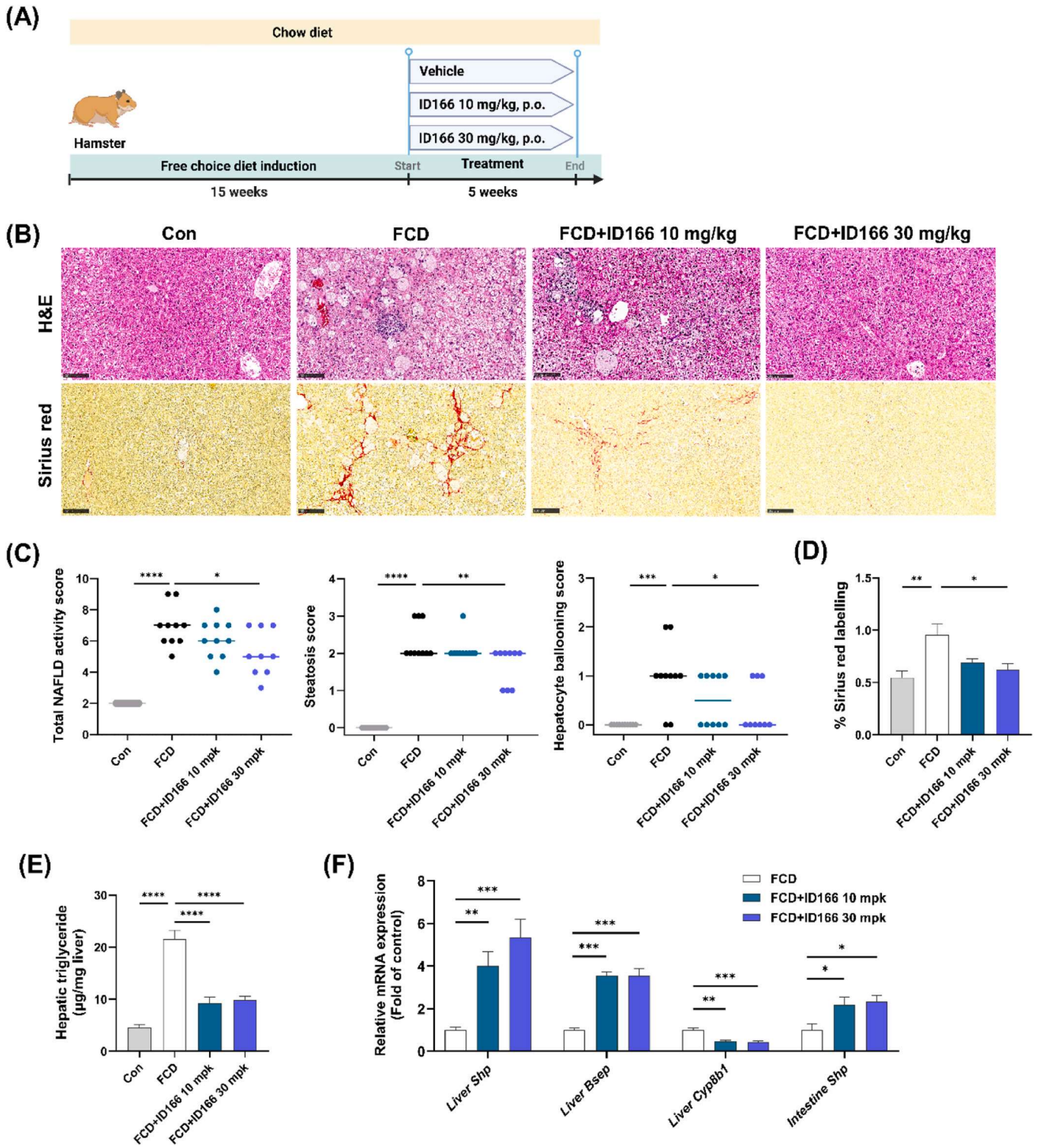

Fig. 2. ID166 ameliorates the NASH phenotype induced by the fed free choice diet. (A) Schematic diagram of the experimental procedure (n=10 for Con, FCD and FCD+ID166 10 mg/kg groups, and n=9 for FCD+ID166 30 mg/kg group). (B) Representative images of hematoxylin-eosin (H&E) and Sirius Red staining in control and NASH hamster liver sections. Scale bar, 100 μm. (C) Total NAFLD activity, steatosis and hepatocyte ballooning scores in control and NASH hamster liver. Data are shown as median. (D) % Sirius Red staining in control and NASH hamster liver. (E) Hepatic TG levels in control and NASH hamsters. (F) Hepatic and intestine mRNA levels of genes related to FXR target engagement in NASH hamsters measured by qPCR. (D-F) Data are presented as mean ± SEM. Significance between control and FCD was determined by Mann-Whitney test. Significant difference between FCD and ID166-treated groups was determined by Kruskal-Wallis with Dunn's post-test. $^{*}p < 0.05$, $^{**}p < 0.01$, $^{***}p < 0.001$ and $^{****}p < 0.0001$ vs FCD. Abbreviations: Con, control; FCD, free choice diet.

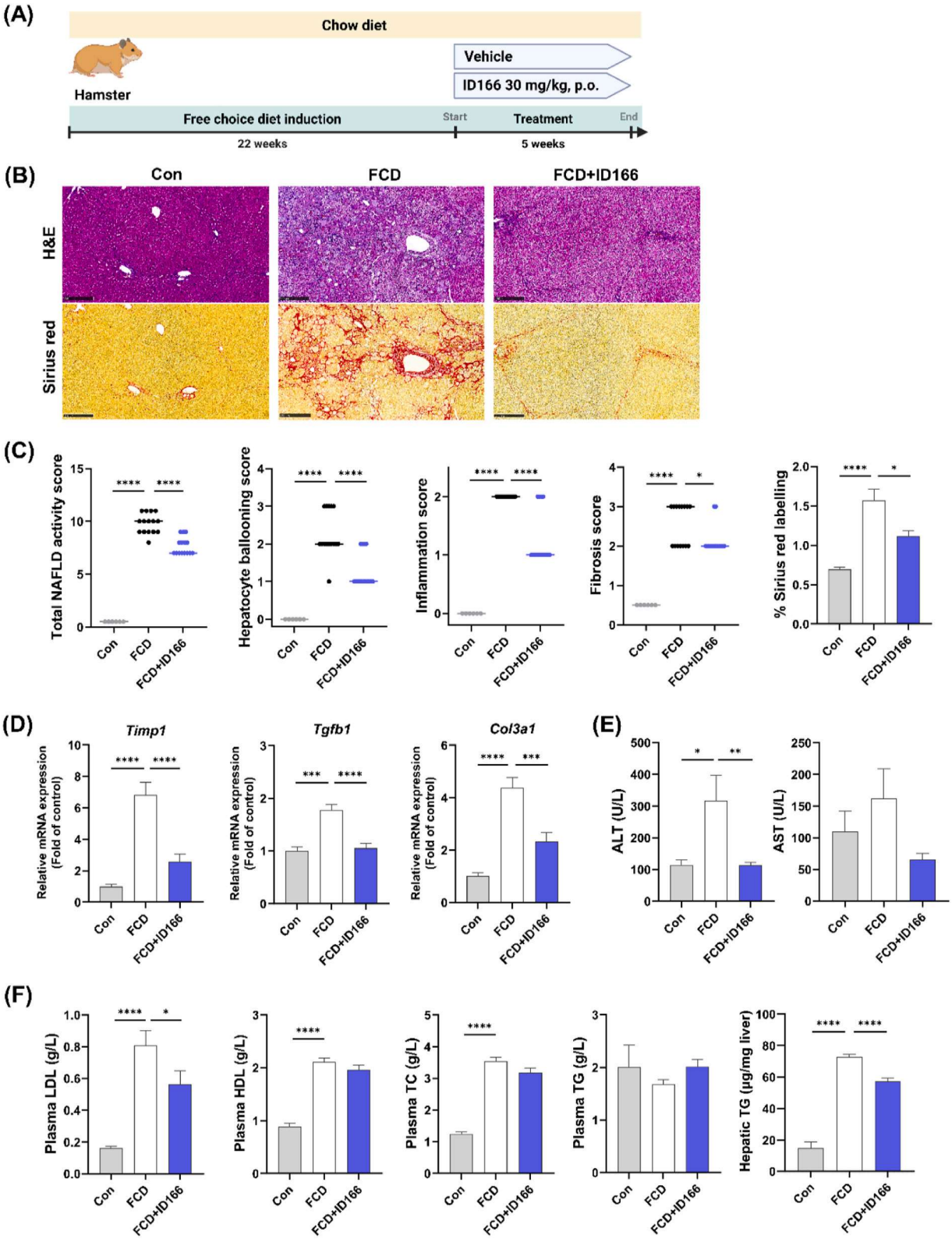

Fig. 3. ID166 reduces total NAFLD activity and hepatic fibrosis score in NASH hamsters fed a free choice diet. (A) Schematic diagram of the experimental procedure (n=6 for Con group, and n=*15* for FCD and FCD+ID166 30 mg/kg groups). (B) Representative image of H&E and Sirius Red staining in control and NASH hamster liver sections. Scale bar, 250 μm. (C) Total NAFLD activity, inflammation, hepatocyte ballooning and fibrosis scores in control and NASH hamster liver are presented as median. % Sirius red labelling in hamster liver is shown as mean ± SEM. (D) Hepatic mRNA levels of fibrogenic genes in control and NASH hamsters. (E) Plasma ALT and AST levels in control and NASH hamsters. (F) Plasma LDL, HDL, TC, TG and hepatic TG levels in control and NASH hamsters. (D-F) Data are presented as mean ± SEM. Significance was determined by Mann-Whitney test and Unpaired t test. $^{*}p < 0.05$, $^{**}p < 0.01$, $^{***}p < 0.001$ and $^{****}p < 0.0001$ vs FCD. Abbreviations: ALT, alanine aminotransferase; AST, aspartate aminotransferase; TG, triglyceride; TC, total cholesterol.

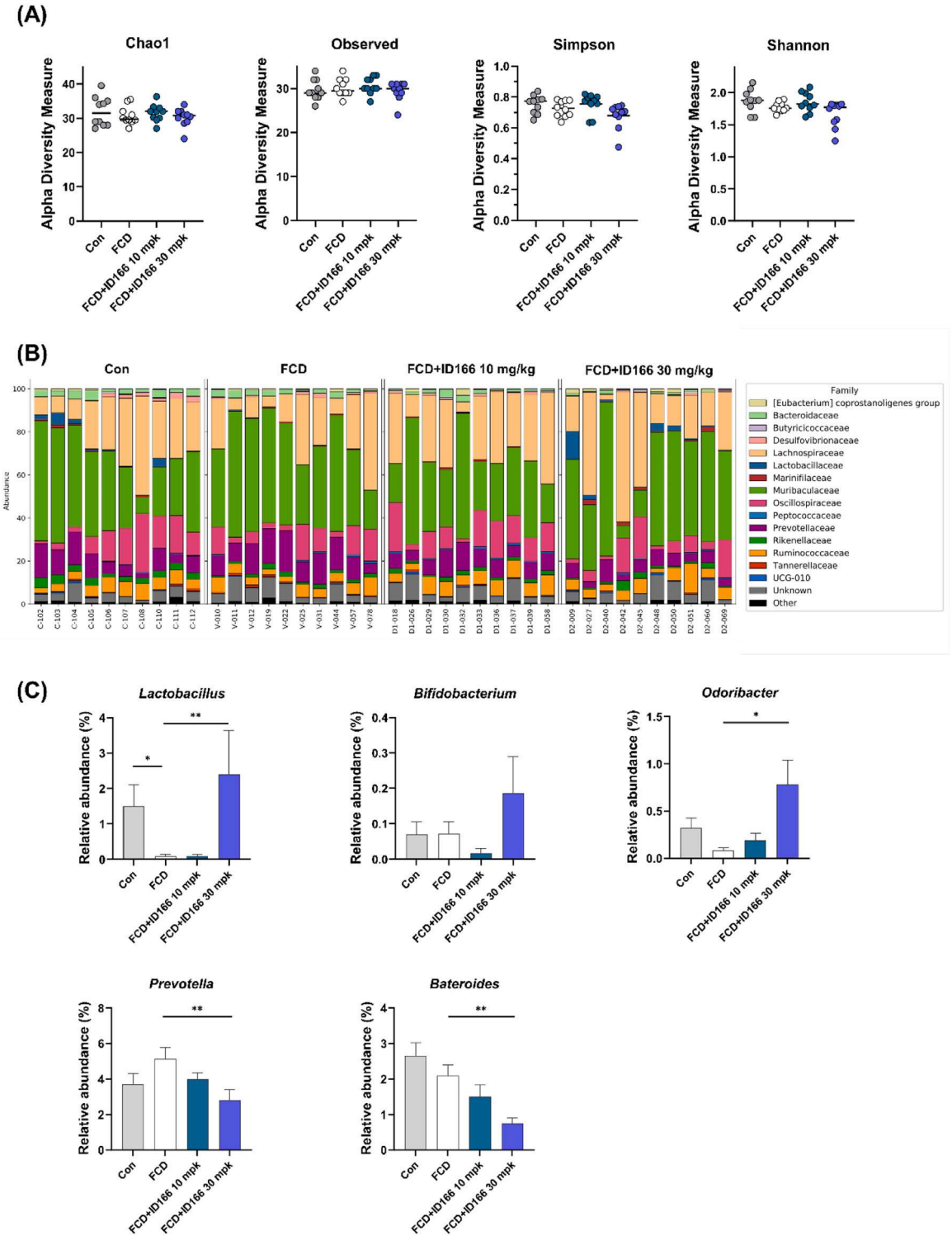

Fig. 4. ID166 preserves the alpha diversity of the gut microbiota in NASH hamsters but induces alterations in the relative abundance of gut microbes. (A) Alpha diversity indices at the family level within fecal samples in control and NASH hamsters (n=10 for Con, FCD and FCD+ID166 10 mg/kg groups, and n=9 for FCD+ID166 30 mg/kg group). (B) The community bar plot analysis depicts the top 15 bacteria at the family level in control and NASH hamsters. (C) The relative abundance of *Lactobacillus*, *Bifidobacterium, Odoribacter, Prevotella* and *Bacteroides* at the genus level in the fecal samples of control and NASH hamsters. Data are presented as Mean ± SEM. Significance was determined by Mann-Whitney test and Kruskal-Wallis with Dunn's post-test. * $p < 0.05$ and ** $p < 0.01$ vs FCD.

conjugated bile acids in NASH hamsters when compared to the hamsters treated with the vehicle (Fig. 5A). Similarly, ID166 treatment significantly reduced total bile acid levels in NASH hamster feces to the level of the control group (Fig. 5B). We also assessed the plasma concentrations of 7α-hydroxy-4-cholesten-3-one (C4), an intermediate product of the classical bile synthesis pathway, which is commonly measured to evaluate the target engagement of FXR agonists in clinical studies.[11] As expected, ID166 showed almost complete reduction of plasma C4 levels in NASH hamsters at 30 mg/kg/day (Fig. 5C). Next, we analyzed detectable primary and secondary bile acid species in plasma. The

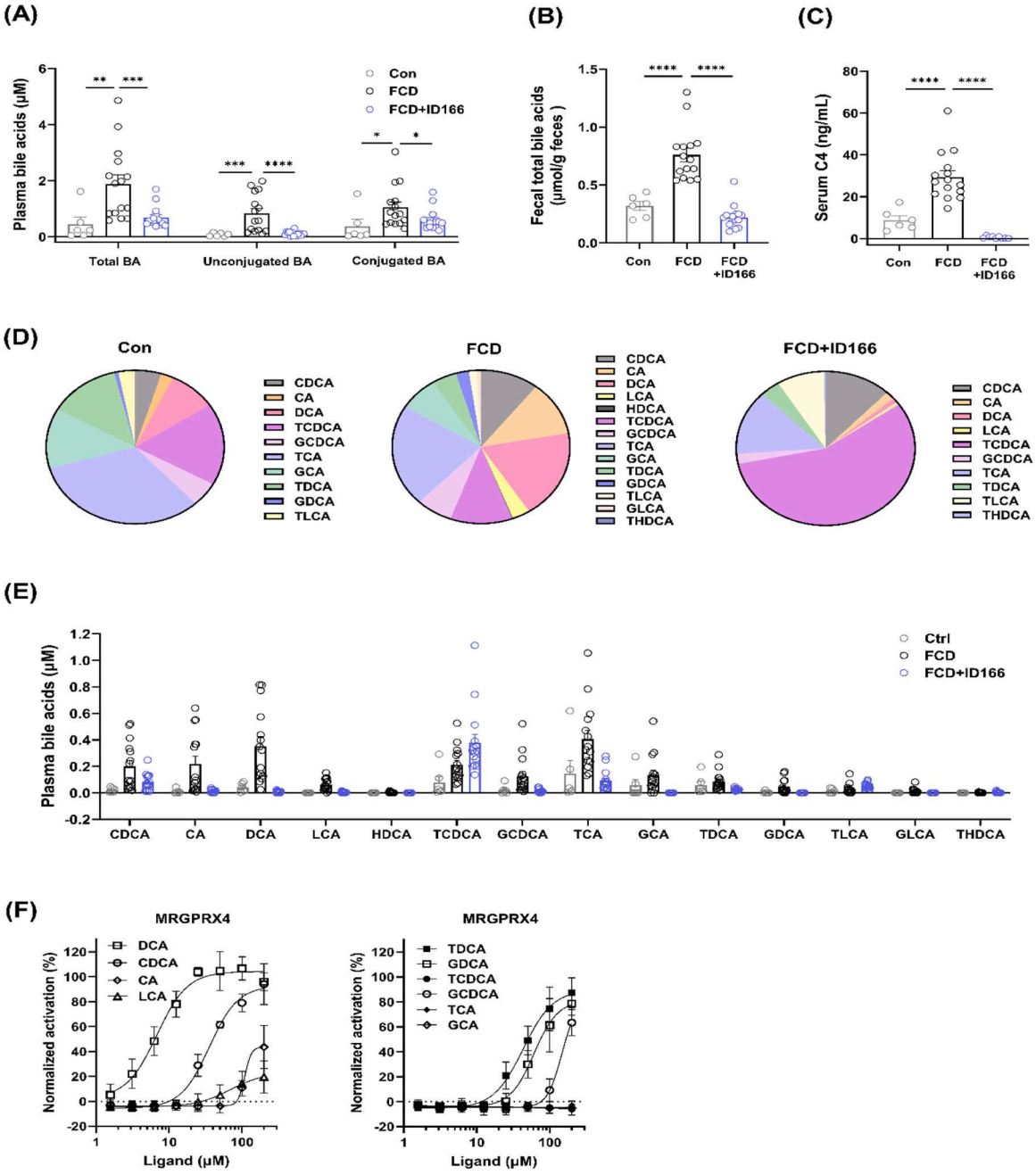

Fig. 5. ID166 reduces the elevated bile acids in NASH hamsters. (A) Plasma concentrations of total, unconjugated and conjugated bile acids (BA) in control and NASH hamsters (n=6 for Con group, and n=15 for FCD and FCD+ID166 groups). (B) Fecal bile acid concentration in control and NASH hamsters. (C) Serum C4 levels in control and NASH hamsters. (D) Composition of plasma bile acids in control and NASH hamsters. (E) Plasma concentrations of measurable bile acid species in control and NASH hamsters. (F) Human MRGPRX4 assay of bile acid species (two independent runs, n=3). Significance was determined by Mann-Whitney test. *p < 0.05, **p < 0.01, ***p < 0.001 and ****p < 0.0001 vs FCD. Abbreviations: C4, 7α-hydroxy-4-cholesten-3-one; CDCA, chenodeoxycholic acid; CA, Cholic acid; LCA, Lithocholic acid; DCA, deoxycholic acid; TDCA, taurodeoxycholic acid; GDCA, glycodeoxycholic acid; TCDCA, taurochenodeoxycholic acid; GCDCA, glycochenodeoxycholic acid; TCA, taurocholic acid; GCA, glycocholic acid; MRGPRX4, Mas-related G protein-coupled receptor X4.

composition of plasma bile acids showed significant differences in each group. In control hamsters, the predominant constituents of the plasma bile acid pool included DCA, TCA, GCA, TCDCA, and TDCA, while in NASH hamsters, CA, CDCA, TCA, TCDCA, and DCA constituted the major plasma bile acids. Notably, in ID166 treated NASH hamsters, TCDCA emerged as the most abundant bile acid species (Fig. 5D). The plasma concentrations of detectable bile acid species were largely different in each group, and DCA and TCA, which exhibited significant increases in the vehicle-treated group, were restored to levels comparable to the control group in the ID166-treated group (Fig. 5E).

Total bile acid levels in human serum were significantly elevated in patients with chronic pruritic disease.[28] Thus, we observed the effect of the 10 bile acid species detected in plasma samples of NASH hamsters on human MRGPRX4. As expected, DCA most potently activated MRGPRX4, and this result is consistent with previous report.[29] Notably, TCDCA, which exhibited significant increases in the ID166-treated group, did not alter the MRGPRX4 activity up to 100 μM (Fig. 5F).

3.5. ID166 reduces diet-induced body weight gain, NASH features and liver fibrosis in HFHC diet-induced obese NASH mice

To assess the long-term efficacy and safety of ID166, mice were orally administered vehicle or two doses of ID166 for 18 weeks after a 7-week induction period on a high fat/high cholesterol (HFHC) diet. In addition to normal hamsters that were fed a chow diet, disease control hamsters were fed an HFHC diet for 25 weeks (Fig. 6A). In contrast to the

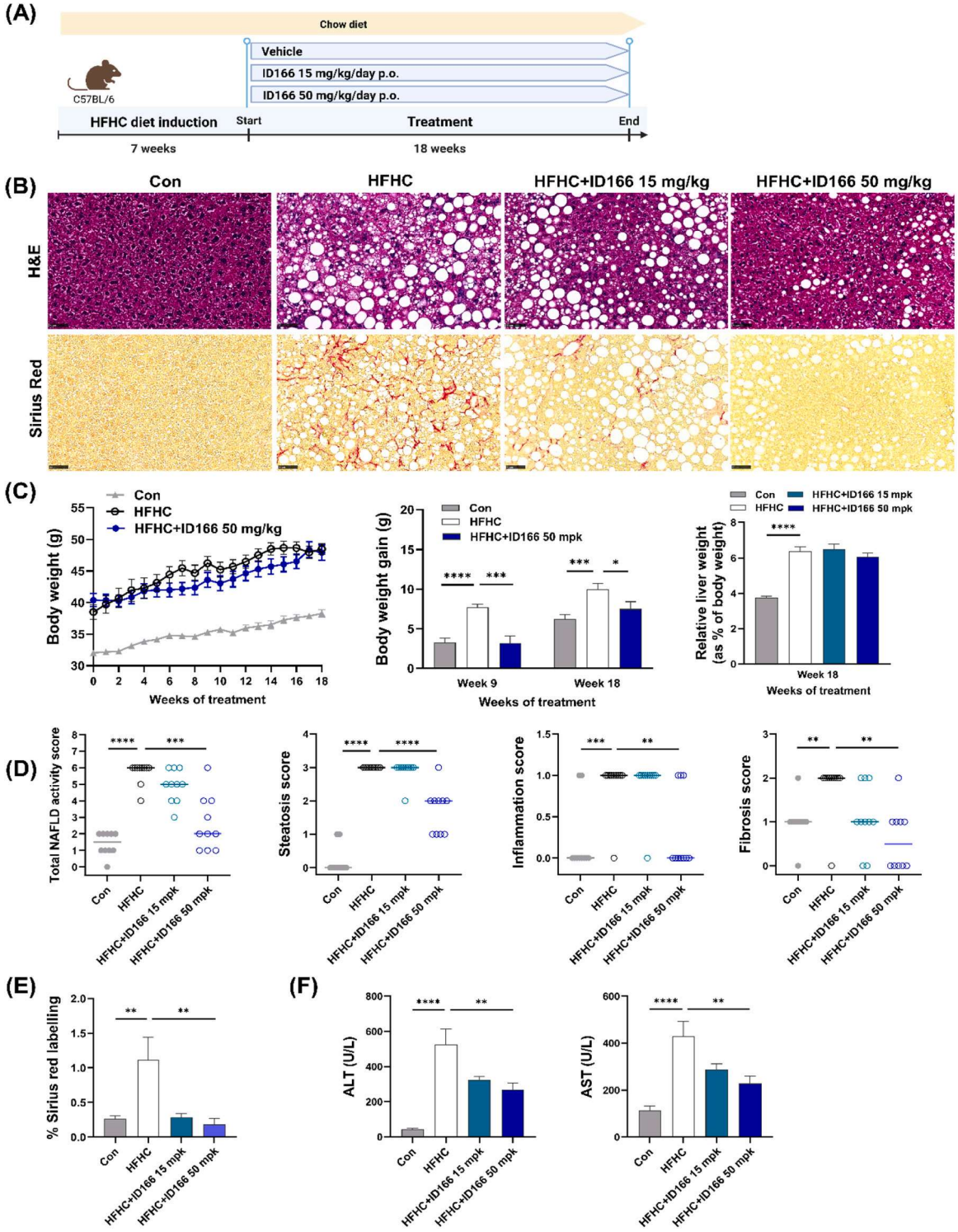

Fig. 6. Long-term treatment with ID166 reduces body weight gain, total NAFLD activity and liver fibrosis in HFHC diet-induced obese NASH mice. (A) Schematic diagram of the experimental procedure ($n=10$ for each group). (B) Representative image of H&E and Sirius Red staining in control and NASH mouse liver sections. Scale bar, 50 μm. (C) Body weight changes and body weight gain at 9 and 18 weeks. Liver weight was measured at week 25 in control and NASH mice. (D) Total NAFLD activity, steatosis, inflammation and fibrosis scores in control and NASH mouse liver. Data are shown as median. (E) % Sirius red labelling in control and NASH mouse liver (mean ± SEM). (F) Plasma ALT and AST levels in control and NASH mice (mean ± SEM). Significance was determined by Mann-Whitney test, Unpaired t test and Kruskal-Wallis with Dunn's post-test. $^{*}p < 0.05$, $^{**}p < 0.01$, $^{***}p < 0.001$ and $^{****}p < 0.0001$ vs HFHC. Abbreviations: HFHC, high fat/high cholesterol.

liver histology of control mice, liver fibrosis was observed in HFHC diet-induced obese NASH mice, and administration of ID166 strongly reduced the liver fibrosis and NASH features in a dose- dependent manner (Fig. 6B). Interestingly, 50 mg/kg/day ID166 considerably reduced diet-induced body weight gain in NASH mice compared to vehicle, but there were no changes in relative liver weight between vehicle and ID166-treated groups (Fig. 6C). 18-week treatment of ID166 at 50 mg/kg/day significantly reduced total NAFLD activity, steatosis, inflammation and fibrosis scores (Fig. 6D). Sirius red staining in NASH mice was also markedly reduced in ID166-treated group compared to vehicle-treated group (Fig. 6E). Plasma ALT and AST levels, which were increased in both disease control and vehicle-treated NASH mice, were significantly reduced in ID166-treated group (Fig. 6F).

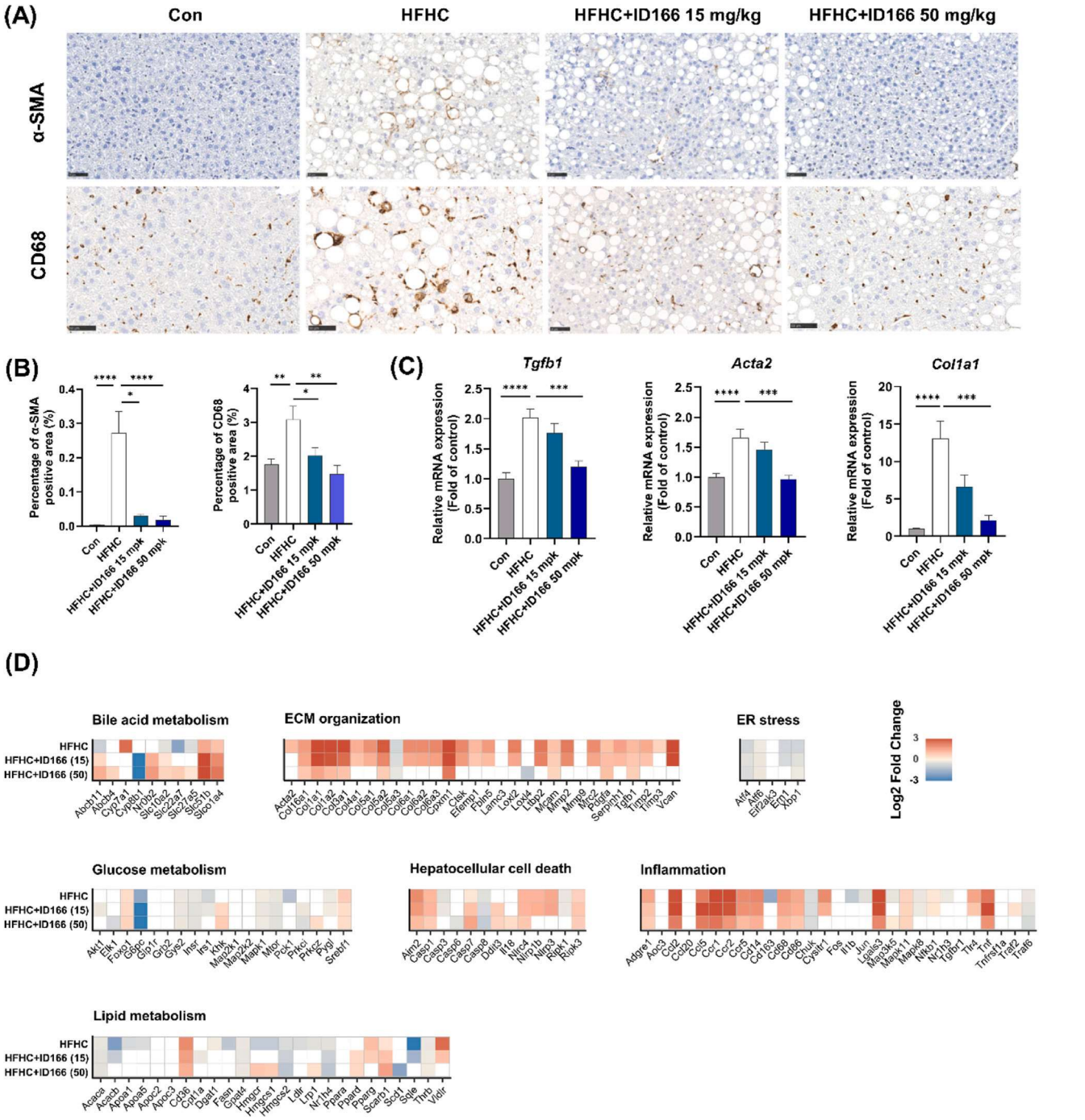

Fig. 7. ID166 modulates protein and gene expression associated with NASH and liver fibrosis in NASH mouse liver. (A) Representative α-SMA and CD68 immunohistochemistry staining in control and NASH mouse liver. Scale bar, 50 μm. (B) α-SMA and CD68-positive liver tissue area in control and NASH mouse liver. (C) mRNA levels of fibrogenic genes in control and NASH mouse liver measured by qPCR. (D) Heatmaps illustrating gene expression changes in NASH and fibrosis-associated genes relative to control in NASH mouse liver (RNAseq analysis). Color gradients in heatmaps indicate significantly upregulated (red color) or down-regulated (blue color) gene expression (log2- fold change, false discovery rate < 0.05). (B-C) n=10 for each group; Significance was determined by Mann-Whitney test, Kruskal-Wallis with Dunn's post-test and one-way ANOVA with Dunnett's post-test. *$p < 0.05$, **$p < 0.01$, ***$p < 0.001$ and ****$p < 0.0001$ vs HFHC. Abbreviations: HFHC, high fat/high cholesterol; ECM, extracellular matrix organization.

3.6. ID166 modulates potential genes linked to NASH and liver fibrosis

Hepatic stellate cells (HSCs) are a major source of extracellular matrix (ECM) to develop liver fibrosis, and alpha-smooth muscle actin (α-SMA) encoded by Acta2 is known to be a widely used HSC marker. [30] In NASH patients, the number of portal cluster of differentiation 68 (CD68)-positive cells were positively correlated with hepatocyte ballooning and lobular inflammation.[31] Thus, we conducted immunohistochemistry (IHC) analysis for α-SMA and CD68 in NASH mouse livers, and found that both α-SMA and CD68 protein levels, which are significantly increased in the liver of NASH mice, were significantly reduced in ID166-treated groups (Fig. 7A, B).

Next, we investigated the gene expression levels of *Tgfb1*, smooth muscle aortic α-actin (*Acta2*), and alpha-1 type I collagen (*Col1a1*). The mRNA expression levels of *Tgfb1*, *Acta2* and *Col1a1* were significantly increased in NASH mice compared to normal mice, and the increased mRNA expression of *Tgfb1*, *Acta2* and *Col1a1* were strongly decreased by ID166 in a dose-dependent manner (Fig. 7C).

Genome-based studies of NASH are becoming increasingly important, and organ-specific gene expression may hold the key to discovering optimum therapy. To obtain in-depth information about the functional mechanisms of ID166 at the molecular level, we performed RNA-seq analysis using normal and NASH mouse liver. In line with α-SMA IHC results, ID166 at 50 mg/kg markedly restored the dysregulated gene expression of extracellular matrix organization, including *Acta2*, *Col1a1*, *Col1a2*, *Col3a1*, *Col5a2*, *Mmp2* and *Timp2*, exhibited in the vehicle-treated group compared to normal mice. Furthermore, as shown in Fig. 7D, ID166 drastically lowered the altered gene expression levels of pro-inflammatory mediators such as *Adgre1*, *Ccl2*, *Ccr5*, *Cd14*, *Cd68*, *Cd86*, *Cysltr1* and *Tlr4* in NASH mouse relative to normal mice. In addition, ID166 altered several genes involved in bile acid metabolism. Because intestinal FXR-mediated FGF15 production is involved in regulating hepatic bile acid synthesis in mice, we observed changes in *Fgf15* gene expression by ID166 in NASH mouse ileum. As expected, the gene expression levels of *Fgf15* were dose-dependently increased by ID166 in NASH mouse ileum (Fig. S3).

3.7. ID166 does not alter scratching behavior and serum IL-31 levels in mice

Although pruritus has been reported as a common side effect in clinical trials of FXR agonists,[9,11,32] the mechanism of action associated with pruritus is not yet fully understood. To examine whether ID166 induces itch in mice, normal BALB/c mice were orally treated with vehicle or 50 mg/kg/day ID166 for 4 weeks. The atopic dermatitis-like skin lesions caused by 2,4-dinitrochlorobenzene (DNCB) exposure were used as disease controls. Unlike the DNCB challenge group, which significantly increased scratching behavior, there was no change in scratching behavior in the ID166-treated group (Fig. 8A).

IL-31 is correlated with serum bile acids levels in NASH patients, and IL-31 mRNA levels are elevated in hepatocytes of NASH patients. Furthermore, IL-31 levels are associated with pruritus, and OCA increases mRNA expression levels of IL-31 in human hepatocytes.[32] IL-31 levels in serum was significantly increased in DNCB challenge group, but there was no significant change in serum concentration of IL-31 in the ID166-treated group (Fig. 8B).

DNCB challenge induced atopic dermatitis-like skin lesions and increased eosinophils and mast cells within the skin lesions, whereas ID166 did not alter the skin tissue (Figs. 8C and 8D).

4. Discussion

Despite the increasing global prevalence of NAFLD across all geographic regions, effective clinical approaches to NASH treatment remain a major challenge.[33,34] FXR agonism has been considered a new approach for NASH treatment, and clinical trials using FXR agonists

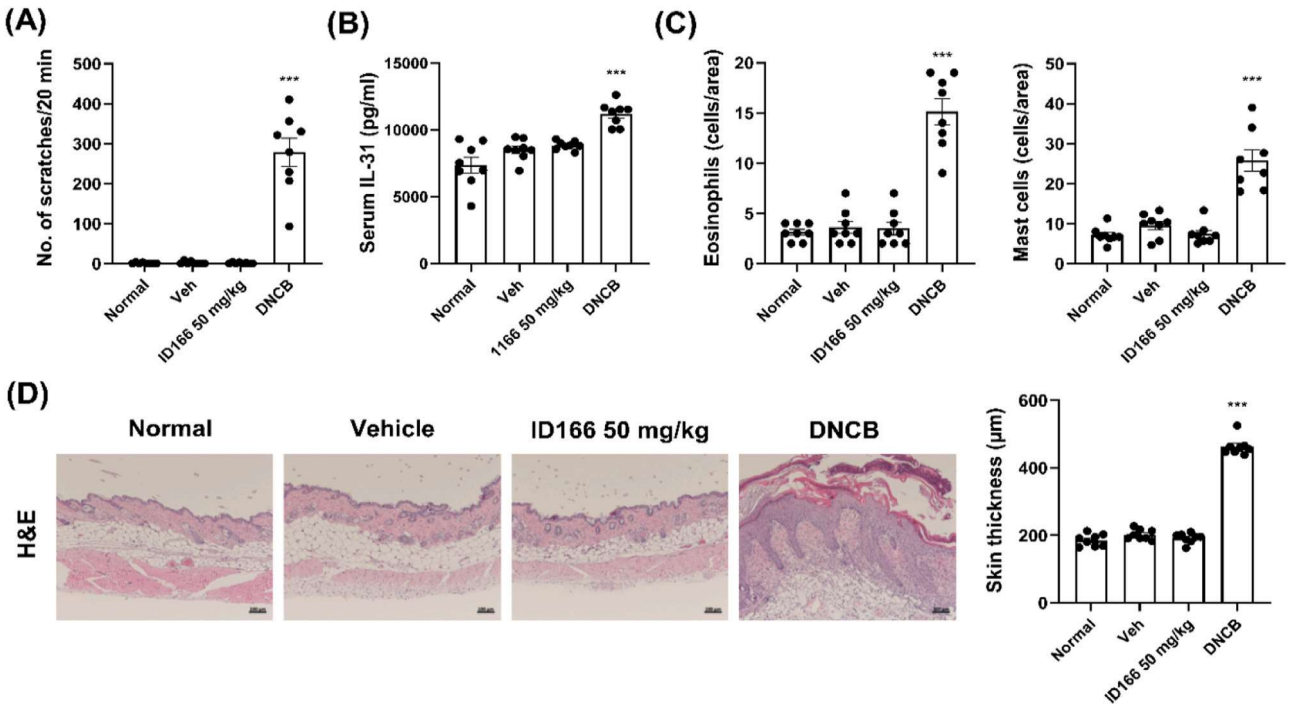

Fig. 8. ID166 has no effects on scratching behavior, serum IL-31 levels, and cutaneous histopathology in mice. (A) Number of scratches in mice was counted during 20 minutes. (B) Serum IL-31 levels in mice. (C) Number of eosinophils (H&E staining) and mast cells (Toluidine blue staining) in mice were quantified. (D) Representative histologic features of cutaneous tissue sections and epidermal thickness in mice. Scale bar, 100 μm. (A-E) Cutaneous DNCB sensitization was performed by applying 1% DNCB on the dorsal skin of the BALB/c mice at Day −7 and Day −4. The BALB/c mice were orally treated with vehicle and 50 mg/kg/day ID166 for 4 weeks. Results were expressed as mean ± SEM and compared by Mann-Whitney test. ***$p < 0.001$ vs Normal ($n=8$ for each group). Abbreviations: DNCB, 2,4-dinitrochlorobenzene.

such as OCA have been attempted. For instance, systemic FXR activation by OCA has demonstrated the initial positive clinical evidence for NASH. However, it has been associated with undesired systemic effects, such as pruritus and elevation in LDL-C levels.[35] Moreover, compared to healthy volunteers, the systemic AUC of total OCA was up to 13-fold higher in subjects with mild to severe liver injury,[36] and considering the liver injuries observed in a subgroup of OCA-treated patients, [37] the persistent overactivation of hepatic FXR may heighten the incidence of liver injury. These results highlight the imperative for the development of new FXR agonists in the treatment of NASH, which can exhibit enhanced effectiveness while minimizing the risk of liver injury. In this study, we examined the effectiveness and mechanism of action of ID166, a novel oral non-bile acid FXR agonist with preferential distribution in the intestine, in animal models of NASH. ID166 is presently undergoing clinical development (NCT05604287).[38]

As shown in Fig. 1D, bile acids such as DCA and LCA potently activate the pruritogenic receptors MRGPRX4 and TGR5, respectively. OCA almost fully activated MRGPRX4 and strongly activated TGR5 with a potency similar to LCA. In addition, previous non-bile acid FXR agonists, such as tropifexor, cilofexor and omesdafexor, partially activated MRGPRX4 (Fig. S4). However, ID166 did not activate MRGPRX4 and TGR5 up to 100 μM. Moreover, in NASH hamster model, ID166 reduced the increased total bile acid plasma levels and especially reduced the plasma concentration of DCA, a strong activator of MRGPRX4, to a lower level than the control group. On the other hand, it significantly increased the plasma concentration of TCDCA, which did not affect the activity of MRGPRX4 (Fig. 5). In addition, repeated administration of ID166 to mouse skin tissue also produced no significant evidence to support FXR agonism-mediated cutaneous events (Fig. 8). In this study, the comprehensive elucidation of the effects of ID166 on itch-related mechanisms was not undertaken. Nevertheless, our findings indicate that ID166, a gut-restricted FXR agonist, is likely to confer an advantage in mitigating itch when compared to previous FXR agonists.

Tissue-specific targeting nuclear receptors including FXR has been attempted to avoid the undesired systemic side effects for NASH.[35] The prolonged gut-biased FXR agonism improves metabolic aberrations and obesity through a sustained increase in the gut hormone FGF19.[12] Notably, serum FGF19 levels in biopsy-proven NAFLD patients were considerably lower than in normal controls and were related to the degree of hepatocyte ballooning.[39] As shown in Fig. 1F, ID166 exhibits a preferential distribution in the intestine. The PK profile and liver concentrations of ID166 showed similar patterns in both NASH hamsters and normal hamsters, and plasma concentrations were maintained relatively well over 24 hours (Fig. S5). We also observed the preferential distribution within the intestine by measuring the time-dependent concentrations of [^{14}C]-ID166 in rat plasma and tissues after single oral administration. Notably, ID166 is distributed at concentrations ~10-fold higher in small intestine compared to the liver and plasma (Fig. S6). In general, drugs with low bioavailability show preferential distribution in the intestines.[40] Evaluation of the bioavailability of ID166 in normal hamsters showed that ID166 had remarkably low oral bioavailability (Table S1). Notably, ID166 substantially increased circulating levels of FGF15, the orthologue of human FGF19, in normal hamsters (Fig. 1E). These results suggest that the tissue distribution profile of ID166 will be useful in confirming the efficacy and safety of tissue-specific FXR activity in future clinical development.

Patients with liver fibrosis exhibited an altered gut microbiota characterized by reduced diversity and richness, increased populations of potentially pathogenic bacteria, and reduced populations of beneficial bacteria.[41] Here, we investigated the effect of ID166 on gut microbiota-bile acid axis in NASH hamster. Interestingly, ID166 significantly reduced the elevated abundance of *Prevotella* and *Bacteroides*, which are associated with obese and NASH,[42] compared to control, and ID166 increased populations of the most widely used traditional probiotics, such as *Lactobacillus* and *Bifidobacterium*. (Fig. 4C). Of note, in patients with NAFLD, probiotics including *Lactobacillus* and *Bifidobacterium* have been demonstrated to have beneficial effects through reductions in serum ALT/AST levels, plasma lipid profile, liver stiffness, and body mass index (BMI).[43,44] Furthermore, *Lactobacillus*, *Bifidobacterium* and *Bacteroides* are the main gut bacteria expressing major bile acid-metabolizing enzymes that can change the bile acid profile,[45] and previous studies revealed that specific plasma bile acid species such as CA, CDCA, GCA, TCA, DCA, TCDCA and GCDCA were significantly higher in NASH patients.[26,27] So, we observed the effect of ID166 on bile acid profile in NASH hamsters. As shown in Fig. 5E, like the changes seen in NASH patients, the plasma levels of CA, CDCA, GCA, TCA, DCA, TCDCA, and GCDCA were increased in NASH hamsters, and the concentrations of all bile acids except TCDCA were reduced to control levels by ID166 treatment. Disruption of the intestinal barrier leads to the systemic translocation of bacteria or bacterial products, contributing to NASH.[46] Although this study did not determine the effect of ID166 on barrier integrity, changes in the expression level of claudin, a tight junction component that plays an important role in controlling barrier permeability, were investigated in NASH mice.[47] Claudin-3 is crucial in the formation of the intestinal barrier's developmental maturation and up-regulation of claudin-8 tightens the epithelium.[48,49] Interestingly, ID166 significantly increased the gene expression levels of claudin-3 and claudin-8 in the ileum of NASH mice compared to vehicle (Fig. S7). This evidence suggests that ID166 may have a protective effect on intestinal barrier integrity. These results strongly suggest that ID166, which is preferentially distributed in the intestine, has an attractive therapeutic potential to beneficially alter the bile acid profile of NASH patients and induce substantial changes in the intestinal microbiota.

Moderate increases in plasma levels of LDL-C would exacerbate the cardiovascular risk for NAFLD patients, who are typically undertreated with lipid-lowering medicines.[50] Increasing evidence indicates that inhibiting cholesteryl ester transfer protein (CETP) leads to elevated HDL-C levels and reduced LDL-C levels.[51] Here, we utilized golden Syrian hamsters expressing CETP to evaluate the effects of ID166 on the lipid profile. As shown in Fig. 3F, ID166 significantly reduced plasma LDL-C levels in NASH hamsters, while OCA increased LDL-C levels in NASH hamster by increasing CETP activity.[22] When we observed the effect of ID166 on the mRNA expression level of CETP, the hepatic mRNA expression level of CETP in NASH hamsters was significantly reduced by ID166 (Fig. S8).

5. Conclusion

ID166 is a novel selective FXR agonist preferentially targeting intestine. Our findings from three different NASH animal models suggest that ID166 effectively improves key histological features of NASH and reduces liver fibrosis. Furthermore, due to its distinct pharmacological profile compared to existing FXR agonists, it is anticipated to improve therapeutic efficacy in NASH clinical trials while minimizing side effects such liver injury and pruritus.

Funding

This study was supported by Ildong pharmaceutical Co., Ltd., Yunovia Co., Ltd. and National Research Foundation of Korea (NRF) grants funded by the Korean government (grant numbers 2018R1A6A1A03023718 to N.W.).

CRediT authorship contribution statement

An-Na Moon: Writing – review & editing, Writing – original draft, Visualization, Investigation, Formal analysis, Conceptualization. **Wan Namkung:** Writing – review & editing, Supervision. **Keonwoo Choi:** Formal analysis. **Yoonsuk Lee:** Supervision. **Martin Rønn Madsen:** Formal analysis. **Hongbin Kim:** Formal analysis. **Natalia Breyner:** Methodology, Investigation. **Dong-Keun Song:** Resources. **François**

Briand: Methodology, Investigation.

Declaration of Competing Interest

An-Na Moon, Dong-Keun Song and Yoonsuk Lee are employed and have shares in iLeadBMS. François Briand and Natalia Breyner are employed in Physiogenex. François Briand have shares in Physiogenex. Martin Rønn Madsen is employed in Gubra. Hongbin Kim and Keonwoo Choi are employed in KINS.

Data availability

The data that support the findings of this study are available from the first author upon reasonable requests.

Acknowledgements

The authors thank all participants from Ildong pharmaceutical and Yunovia for their intellectual contributions, molecular docking simulation and financial support. BioRender was used to construct the schematic figures after obtaining a paid license for publication authorization.

Appendix A. Supporting information

Supplementary data associated with this article can be found in the online version at doi:10.1016/j.biopha.2024.116331.

References

[1] Z.M. Younossi, M. Stepanova, J. Ong, G. Trimble, S. AlQahtani, I. Younossi, A. Ahmed, A. Racila, L. Henry, Nonalcoholic steatohepatitis is the most rapidly increasing indication for liver transplantation in the United States, e585, Clin. Gastroenterol. Hepatol. 19 (3) (2021) 580–589, https://doi.org/10.1016/j.cgh.2020.05.064.

[2] Z. Younossi, P. Aggarwal, I. Shrestha, J. Fernandes, P. Johansen, M. Augusto, S. Nair, The burden of non-alcoholic steatohepatitis: A systematic review of health-related quality of life and patient-reported outcomes, JHEP Rep. (2022) 100525, https://doi.org/10.1016/j.jhepr.2022.100525.

[3] J.M. Paik, K. Kabbara, K.E. Eberly, Y. Younossi, L. Henry, Z.M. Younossi, Global burden of NAFLD and chronic liver disease among adolescents and young adults, Hepatology 75 (5) (2022) 1204–1217, https://doi.org/10.1002/hep.32228.

[4] D. Ferguson, B.N. Finck, Emerging therapeutic approaches for the treatment of NAFLD and type 2 diabetes mellitus, Nat. Rev. Endocrinol. 17 (8) (2021) 484–495, https://doi.org/10.1038/s41574-021-00507-z.

[5] H. Wang, J. Chen, K. Hollister, L.C. Sowers, B.M. Forman, Endogenous bile acids are ligands for the nuclear receptor FXR/BAR, Mol. Cell 3 (5) (1999) 543–553, https://doi.org/10.1016/s1097-2765(00)80348-2.

[6] Y. Zhang, H.R. Kast-Woelbern, P.A. Edwards, Natural structural variants of the nuclear receptor farnesoid X receptor affect transcriptional activation, J. Biol. Chem. 278 (1) (2003) 104–110, https://doi.org/10.1074/jbc.M209505200.

[7] Y.-D. Wang, W.-D. Chen, D.D. Moore, W. Huang, FXR: a metabolic regulator and cell protector, Cell Res. 18 (11) (2008) 1087–1095, https://doi.org/10.1038/cr.2008.289.

[8] M. Wagner, G. Zollner, M. Trauner, Nuclear receptors in liver disease, Hepatology 53 (3) (2011) 1023–1034, https://doi.org/10.1002/hep.24148.

[9] Z.M. Younossi, V. Ratziu, R. Loomba, M. Rinella, Q.M. Anstee, Z. Goodman, P. Bedossa, A. Geier, S. Beckebaum, P.N. Newsome, Obeticholic acid for the treatment of non-alcoholic steatohepatitis: interim analysis from a multicentre, randomised, placebo-controlled phase 3 trial, Lancet 394 (10215) (2019) 2184–2196, https://doi.org/10.1016/S0140-6736(19)33041-7.

[10] D.C. Tully, P.V. Rucker, D. Chianelli, J. Williams, A. Vidal, P.B. Alper, D. Mutnick, B. Bursulaya, J. Schmeits, X. Wu, D. Bao, J. Zoll, Y. Kim, T. Groessl, P. McNamara, H.M. Seidel, V. Molteni, B. Liu, A. Phimister, S.B. Joseph, B. Laffitte, Discovery of Tropifexor (LJN452), a Highly Potent Non-bile Acid FXR Agonist for the Treatment of Cholestatic Liver Diseases and Nonalcoholic Steatohepatitis (NASH), J. Med. Chem. 60 (24) (2017) 9960–9973, https://doi.org/10.1021/acs.jmedchem.7b00907.

[11] A.J. Sanyal, P. Lopez, E.J. Lawitz, K.J. Lucas, J. Loeffler, W. Kim, G.B.B. Goh, J. F. Huang, C. Serra, P. Andreone, Y.C. Chen, S.H. Hsia, V. Ratziu, D. Aizenberg, H. Tobita, A.M. Sheikh, J.M. Vierling, Y.J. Kim, H. Hyogo, D. Tai, Z. Goodman, F. Schaefer, I.R.I. Carbarns, S. Lamle, M. Martic, N.V. Naoumov, C.A. Brass, Tropifexor for nonalcoholic steatohepatitis: an adaptive, randomized, placebo-controlled phase 2a/b trial, Nat. Med. 29 (2) (2023) 392–400, https://doi.org/10.1038/s41591-022-02200-8.

[12] S. Fang, J.M. Suh, S.M. Reilly, E. Yu, O. Osborn, D. Lackey, E. Yoshihara, A. Perino, S. Jacinto, Y. Lukasheva, Intestinal FXR agonism promotes adipose tissue browning and reduces obesity and insulin resistance, Nat. Med. 21 (2) (2015) 159–165, https://doi.org/10.1038/nm.3760.

[13] S.A. Harrison, M.R. Bashir, J. Shim-Lopez, K. Song, H.C. Chen, MET409, a sustained FXR agonist, decreased hepatic fat and improved liver function without raising LDL-C after 28 days in NASH patients, Hepatology 70 (Suppl) (2019) 1257A.

[14] S.A. Harrison, M.R. Bashir, K.-J. Lee, J. Shim-Lopez, J. Lee, B. Wagner, N.D. Smith, H.C. Chen, E.J. Lawitz, A structurally optimized FXR agonist, MET409, reduced liver fat content over 12 weeks in patients with non-alcoholic steatohepatitis, J. Hepatol. 75 (1) (2021) 25–33.

[15] S. Lang, B. Schnabl, Microbiota and fatty liver disease—the known, the unknown, and the future, Cell Host Microbe 28 (2) (2020) 233–244, https://doi.org/10.1016/j.chom.2020.07.007.

[16] J. Boursier, O. Mueller, M. Barret, M. Machado, L. Fizanne, F. Araujo-Perez, C. D. Guy, P.C. Seed, J.F. Rawls, L.A. David, The severity of nonalcoholic fatty liver disease is associated with gut dysbiosis and shift in the metabolic function of the gut microbiota, Hepatology 63 (3) (2016) 764–775, https://doi.org/10.1002/hep.28356.

[17] S.I. Sayin, A. Wahlström, J. Felin, S. Jäntti, H.-U. Marschall, K. Bamberg, B. Angelin, T. Hyötyläinen, M. Orešič, F. Bäckhed, Gut microbiota regulates bile acid metabolism by reducing the levels of tauro-beta-muricholic acid, a naturally occurring FXR antagonist, Cell Metab. 17 (2) (2013) 225–235, https://doi.org/10.1016/j.cmet.2013.01.003.

[18] Moon A.-N., Lee Y., Song D.–K., Briand F. ID119031166, A Novel Potent Non-bile acid FXR Agonist, Improves NASH and Liver Fibrosis Without Plasma LDL-C Elevation in a Diet-induced Obese NASH Hamster Model. In.HEPATOLOGY: WILEY 111 RIVER ST, HOBOKEN 07030-5774, NJ USA; 2022. p. S611-S611.

[19] C. Cao, H.J. Kang, I. Singh, H. Chen, C. Zhang, W. Ye, B.W. Hayes, J. Liu, R. H. Gumpper, B.J. Bender, Structure, function and pharmacology of human itch GPCRs, Nature 600 (7887) (2021) 170–175, https://doi.org/10.1038/s41586-021-04126-6.

[20] V. Sepe, E. Distrutti, S. Fiorucci, A. Zampella, Farnesoid X receptor modulators (2011–2014): a patent review, Expert Opin. Ther. Pat. 25 (8) (2015) 885–896, https://doi.org/10.1517/13543776.2015.1045413.

[21] C. Gege, O. Kinzel, C. Steeneck, A. Schulz, C. Kremoser, Knocking on FXR´s Door: The, Curr. Top. Med. Chem. 14 (19) (2014) 2143–2158, https://doi.org/10.2174/1568026614666141112094430.

[22] F. Briand, E. Brousseau, M. Quinsat, R. Burcelin, T. Sulpice, Obeticholic acid raises LDL-cholesterol and reduces HDL-cholesterol in the Diet-Induced NASH (DIN) hamster model, Eur. J. Pharm. 818 (2018) 449–456, https://doi.org/10.1016/j.ejphar.2017.11.021.

[23] F. Briand, J. Maupoint, E. Brousseau, N. Breyner, M. Bouchet, C. Costard, T. Leste-Lasserre, M. Petitjean, L. Chen, A. Chabrat, Elafibranor improves diet-induced nonalcoholic steatohepatitis associated with heart failure with preserved ejection fraction in Golden Syrian hamsters, Metabolism 117 (2021) 154707, https://doi.org/10.1016/j.metabol.2021.154707.

[24] M. Ouimet, T.J. Barrett, E.A. Fisher, HDL and reverse cholesterol transport: Basic mechanisms and their roles in vascular health and disease, Circ. Res. 124 (10) (2019) 1505–1518, https://doi.org/10.1161/CIRCRESAHA.119.312617.

[25] K. Tsutsumi, A. Hagi, Y. Inoue, The relationship between plasma high density lipoprotein cholesterol levels and cholesteryl ester transfer protein activity in six species of healthy experimental animals, Biol. Pharm. Bull. 24 (5) (2001) 579–581, https://doi.org/10.1248/bpb.24.579.

[26] G. Grzych, O. Chávez-Talavera, A. Descat, D. Thuillier, A. Verrijken, M. Kouach, V. Legry, H. Verkindt, V. Raverdy, B. Legendre, NASH-related increases in plasma bile acid levels depend on insulin resistance, JHEP Rep. 3 (2) (2021) 100222.

[27] P. Puneet, P. Puri, K. Daita, A. Joyce, F. Mirshahi, P.K. Santhekadur, S. Cazanave, V.A. Luketic, M.S. Siddiqui, S. Boyett, H.K. Min, D.P. Kumar, R. Kohli, H. Zhou, P. B. Hylemon, M.J. Contos, M. Idowu, A.J. Sanyal, The presence and severity of nonalcoholic steatohepatitis is associated with specific changes in circulating bile acids, 534-, In (2018) 534–548, https://doi.org/10.1002/hep.29359.

[28] K. Eisendle, H. Müller, E. Ortner, H. Talasz, I. Graziadei, W. Vogel, R. Höpfl, Pruritus of unknown origin and elevated total serum bile acid levels in patients without clinically apparent liver disease, J. Gastroenterol. Hepatol. 26 (4) (2011) 716–721, https://doi.org/10.1111/j.1440-1746.2010.06522.x.

[29] J. Meixiong, C. Vasavda, S.H. Snyder, X. Dong, MRGPRX4 is a G protein-coupled receptor activated by bile acids that may contribute to cholestatic pruritus, Proc. Natl. Acad. Sci. 116 (21) (2019) 10525–10530, https://doi.org/10.1073/pnas.1903316116.

[30] I. Mederacke, C.C. Hsu, J.S. Troeger, P. Huebener, X. Mu, D.H. Dapito, J.-P. Pradere, R.F. Schwabe, Fate tracing reveals hepatic stellate cells as dominant contributors to liver fibrosis independent of its aetiology, Nat. Commun. 4 (1) (2013) 2823, https://doi.org/10.1038/ncomms3823.

[31] V.L. Gadd, R. Skoien, E.E. Powell, K.J. Fagan, C. Winterford, L. Horsfall, K. Irvine, A.D. Clouston, The portal inflammatory infiltrate and ductular reaction in human nonalcoholic fatty liver disease, Hepatology 59 (4) (2014) 1393–1405, https://doi.org/10.1002/hep.26937.

[32] J. Xu, Y. Wang, M. Khoshdeli, M. Peach, J.C. Chuang, J. Lin, W.W. Tsai, S. Mahadevan, W. Minto, L. Diehl, IL-31 levels correlate with pruritus in patients with cholestatic and metabolic liver diseases and is farnesoid X receptor responsive in NASH, Hepatology (2022), https://doi.org/10.1002/hep.32599.

[33] Z.M. Younossi, P. Golabi, J.M. Paik, A. Henry, C. Van Dongen, L. Henry, The global epidemiology of nonalcoholic fatty liver disease (NAFLD) and nonalcoholic steatohepatitis (NASH): a systematic review, Hepatology 77 (4) (2023) 1335–1347, https://doi.org/10.1097/HEP.0000000000000004.

[34] S.A. Harrison, A.M. Allen, J. Dubourg, M. Noureddin, N. Alkhouri, Challenges and opportunities in NASH drug development, Nat. Med 29 (3) (2023) 562–573, https://doi.org/10.1038/s41591-023-02242-6.
[35] Z. Henry, V. Meadows, G.L. Guo, FXR and NASH: an avenue for tissue-specific regulation, Hepatol. Commun. 7 (5) (2023), https://doi.org/10.1097/HC9.0000000000000127.
[36] J. Edwards, C. LaCerte, T. Peyret, N. Gosselin, J. Marier, A. Hofmann, D. Shapiro, Modeling and experimental studies of obeticholic acid exposure and the impact of cirrhosis stage, Clin. Transl. Sci. 9 (6) (2016) 328–336, https://doi.org/10.1111/cts.12421.
[37] J.E. Eaton, R. Vuppalanchi, R. Reddy, S.K. Satapathy, B. Ali, P.S. Kamath, Liver injury in patients with cholestatic liver disease treated with obeticholic acid, Hepatology 71 (4) (2020) 1511–1514, https://doi.org/10.1002/hep.31017.
[38] Safety, Tolerability, and Pharmacokinetics of ID119031166M With the Exploration of Pharmacodynamic Effects. In.: ⟨https://classic.clinicaltrials.gov/show/NCT05604287⟩.
[39] F. Eren, R. Kurt, F. Ermis, O. Atug, N. Imeryuz, Y. Yilmaz, Preliminary evidence of a reduced serum level of fibroblast growth factor 19 in patients with biopsy-proven nonalcoholic fatty liver disease, Clin. Biochem. 45 (9) (2012) 655–658, https://doi.org/10.1016/j.clinbiochem.2012.03.019.
[40] R. Dorel, A.R. Wong, J.J. Crawford, Trust your gut: strategies and tactics for intestinally restricted drugs, ACS Med. Chem. Lett. 14 (3) (2023) 233–243.
[41] Y.-L. Zhang, Z.-J. Li, H.-Z. Gou, X.-J. Song, L. Zhang, The gut microbiota–bile acid axis: a potential therapeutic target for liver fibrosis, Front. Cell. Infect. Microbiol. 12 (2022), https://doi.org/10.3389/fcimb.2022.945368.
[42] L. Zhu, S.S. Baker, C. Gill, W. Liu, R. Alkhouri, R.D. Baker, S.R. Gill, Characterization of gut microbiomes in nonalcoholic steatohepatitis (NASH) patients: a connection between endogenous alcohol and NASH, Hepatology 57 (2) (2013) 601–609, https://doi.org/10.1002/hep.26093.
[43] E. Manzhalii, O. Virchenko, T. Falalyeyeva, T. Beregova, W. Stremmel, Treatment efficacy of a probiotic preparation for non-alcoholic steatohepatitis: a pilot trial, J. Dig. Dis. 18 (12) (2017) 698–703, https://doi.org/10.1111/1751-2980.12561.
[44] F. Famouri, Z. Shariat, M. Hashemipour, M. Keikha, R. Kelishadi, Effects of probiotics on nonalcoholic fatty liver disease in obese children and adolescents, J. Pediatr. Gastroenterol. Nutr. 64 (3) (2017) 413–417, https://doi.org/10.1097/MPG.0000000000001422.
[45] E. Smirnova, M.D. Muthiah, N. Narayan, M.S. Siddiqui, P. Puri, V.A. Luketic, M. J. Contos, M. Idowu, J.C. Chuang, A.N. Billin, Metabolic reprogramming of the intestinal microbiome with functional bile acid changes underlie the development of NAFLD, Hepatology 76 (6) (2022) 1811–1824, https://doi.org/10.1002/hep.32568.
[46] J. Mouries, P. Brescia, A. Silvestri, I. Spadoni, M. Sorribas, R. Wiest, E. Mileti, M. Galbiati, P. Invernizzi, L. Adorini, Microbiota-driven gut vascular barrier disruption is a prerequisite for non-alcoholic steatohepatitis development, J. Hepatol. 71 (6) (2019) 1216–1228.
[47] Z. Lu, L. Ding, Q. Lu, Y.-H. Chen, Claudins in intestines: distribution and functional significance in health and diseases, Tissue Barriers 1 (3) (2013) e24978.
[48] R.M. Patel, L.S. Myers, A.R. Kurundkar, A. Maheshwari, A. Nusrat, P.W. Lin, Probiotic bacteria induce maturation of intestinal claudin 3 expression and barrier function, Am. J. Pathol. 180 (2) (2012) 626–635.
[49] S. Amasheh, S. Milatz, S.M. Krug, A.G. Markov, D. Günzel, M. Amasheh, M. Fromm, Tight junction proteins as channel formers and barrier builders: claudin-2,-5, and-8, Ann. N. Y. Acad. Sci. 1165 (1) (2009) 211–219.
[50] C. Labenz, J.H. Prochaska, Y. Huber, M. Nagel, B.K. Straub, P. Wild, P.R. Galle, J. M. Schattenberg, Cardiovascular risk categories in patients with nonalcoholic fatty liver disease and the role of Low-Density lipoprotein cholesterol, Hepatol. Commun. 3 (11) (2019) 1472–1481, https://doi.org/10.1002/hep4.1428.
[51] S.J. Nicholls, M. Ditmarsch, J.J. Kastelein, S.P. Rigby, D. Kling, D.L. Curcio, N. J. Alp, M.H. Davidson, Lipid lowering effects of the CETP inhibitor obicetrapib in combination with high-intensity statins: a randomized phase 2 trial, Nat. Med. 28 (8) (2022) 1672–1678, https://doi.org/10.1038/s41591-022-01936-7.